



PHASE EQUILIBRIUM DATA AND THERMODYNAMIC MODELING OF THE SYSTEM R-1234yf AND POLYOL ESTER LUBRICANT OIL

Rafael Massabki França
Moisés A. Marcelino Neto
Jader R. Barbosa Jr.

POLO-Research Laboratories for Emerging Technologies in Cooling and Thermophysics, Department of Mechanical Engineering, Federal University of Santa Catarina, Florianópolis-SC, 88040900, Brazil
moises@polo.ufsc.br

Abstract. In recent years, research and development of the so-called fourth generation refrigerants (with zero ozone depletion potential, ODP, and low global warming potential, GWP) are a significant part of the effort to deal with global warming due to atmospheric release of greenhouse gases. 2,3,3,3-tetrafluoroprop-1-ene (R-1234yf) is a new synthetic low-GWP refrigerant designed to act as a drop-in replacement for R-134a. Detailed knowledge of the phase equilibrium behavior of refrigerant/lubricant systems is fundamental to properly design refrigeration compressors. The main objective of this work is to investigate the phase behavior of the system R-1234yf/polyol ester (POE) ISO VG 10 lubricant. For comparison purposes, the phase behavior of the R-134a/POE ISO VG 10 was also characterized. The static synthetic method using a variable-volume PVT cell was employed to obtain experimental data between 13°C and 80°C, with pressures up to 2.5 MPa. For both systems, vapor-liquid equilibrium was observed over the entire temperature range. The data were correlated via the Peng and Robinson (1976) equation of state with the classical van der Waals mixing rule, with 0.75 and 0.74% RMS error for the R-1234yf and R-134a mixtures, respectively.

Keywords: phase equilibrium, R-1234yf, R-134a, polyol ester oil, thermodynamic model

1. INTRODUCTION

Refrigerants with low Global Warming Potential (GWP) have been the focus of many research works over the past decades. In current mobile air conditioning (MAC) systems, the most popular refrigerant is 1,1,1,2-tetrafluoroethane (R-134a), but its GWP of 1300 is considered too large under the current European regulations (Zilio *et al.*, 2011). R-134a is also widely used as a refrigerant in domestic and light commercial applications. A new synthetic chemical, R-1234yf (2,3,3,3-tetrafluoroprop-1-ene), was identified as a potential drop-in replacement for R-134a in such systems, depending on its compatibility with the lubricant oil and other materials (seals, gaskets etc.) originally in place. R-1234yf has a GWP of around 4, zero Ozone Depletion Potential (ODP) and vapor pressure and other properties similar to those of HFC-134a.

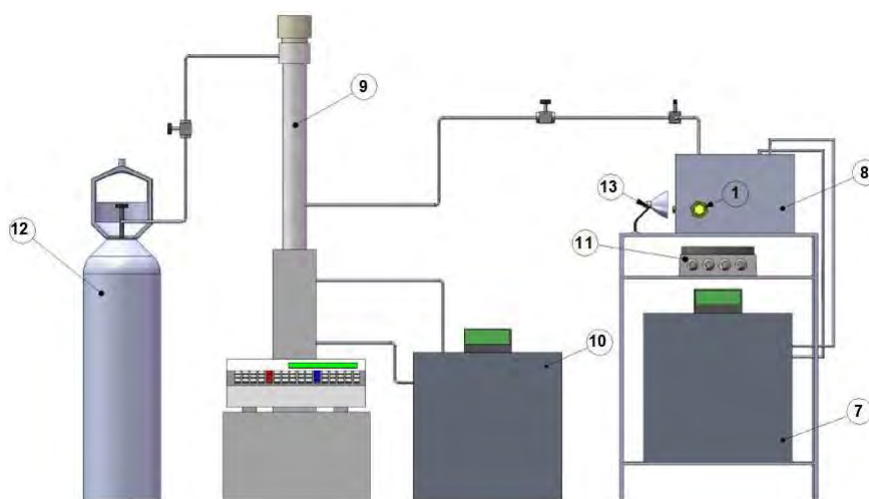
Despite its importance in compressor design for small capacity cooling systems, there is a lack of experimental data in the open literature dealing the the phase behavior of R-1234yf/Polyol Ester (POE) oil mixtures. Limited data on the partial miscibility of R-1234yf with POE lubricants have been presented by Leck (2009). Spatz (2009) presented a diagram showing a miscibility gap of some PAG lubricants. Bobbo *et al.* (2011) presented solubility data in terms of pressure as a function of R-1234yf mass fraction in a Polyalkylene Glycol (PAG) commercial lubricant. The authors characterized the phase equilibria by means of a static synthetic method at isothermal conditions in the temperature range between -15°C and 65°C. At temperatures higher than 20°C, the system showed a miscibility gap, i.e. the formation of a second liquid phase, richer in R-1234yf, at equilibrium. This behavior was not observed for the R-134a/PAG system at 20°C, highlighting a possible problem in the use of R-1234yf if PAG lubricants were selected for the applications.

As phase equilibrium data for R-1234yf/oil mixtures are still scarce in the literature, the present study has been dedicated to the experimental determination of the pressure-temperature-composition behavior of the mixture in the temperature range between 13°C and 80°C. In addition to comparing the behavior of R-1234yf and R-134a in terms of their interaction with the lubricant oil, phase equilibrium experiments were also conducted for R-134a. The phase equilibrium data obtained were modeled using the Peng and Robinson (1976) equation of state with the classical van der Waals mixing rule.

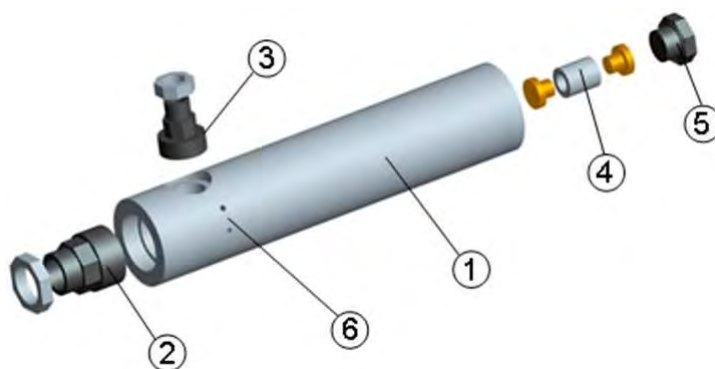
2. EXPERIMENTS

Phase equilibria of the R-1234yf and R-134a/POE ISO VG 10 mixtures were measured in the experimental apparatus shown in Fig. 1a. The equilibrium cell (1), illustrated in Fig. 1b, is an AISI 316L stainless steel pressure vessel of 230 mm in length and 17 mm ID. Inside the cell, a moving piston (4) divides the internal volume into two chambers (front and rear). The front chamber, which is the actual PVT cell, is equipped with two sapphire windows (2) and (3) for visual inspection of the fluid mixture. The rear chamber is sealed with a back plug (5). Both chambers are connected to a syringe pump (9) that is connected to the POE ISO VG 10 reservoir (12). The front chamber has two additional ports (6); one for

temperature measurement with a Pt-100 RTD ($\pm 0.15^\circ\text{C}$ uncertainty), and another for fluid charging and absolute pressure measurement (uncertainty of ± 0.15 bar). The temperature of the system is set by a thermostatic bath (7) that circulates service water through a tank (8) where the equilibrium cell (1) is located. The syringe pump controls the pressure and the mixture concentration in the front chamber, as will be explained below. The temperature in the pump is controlled by a second thermostatic bath (10).



(a) System components.



(b) PVT cell.

Figure 1. Schematic diagram of the experimental apparatus.

The experimental procedure to determine the bubble point pressure as a function of temperature and overall composition is described as follows. Initially, the syringe pump is charged with oil and a 0.04-mbar vacuum is made in the internal pump circuit. The desired temperature is set in the thermostatic bath (10) and the pump is pressurized. A specified amount of refrigerant (measured with the help of a precision balance) is inserted in the previously evacuated front chamber and the cell is placed inside the tank (8). Next, a 0.04-mbar vacuum is made in the rear chamber and remaining connecting lines. The desired overall composition in the PVT cell is set by opening the feeding valve connected to port (6) and slowly pumping a predefined amount of oil into the front chamber. During this process, no pressure is applied to the rear face of the piston. The mixture in the PVT cell is agitated with a magnetic stirrer (11) and the thermostatic bath (7) is switched on.

When the desired system temperature is reached, the rear chamber is pressurized using the syringe pump (the lubricant oil itself is the hydraulic fluid) until it is ensured (by visual inspection) that only a liquid phase exists in the PVT cell (point A_1 in Fig. 2). At a constant temperature and with the magnetic stirrer on, the piston is moved towards the rear to start a gradual decrease in pressure. The slow depressurization rate is maintained until the appearance of a second phase (vapor bubbles) and, at the slightest sign of this phase transition (point B_1 in Fig. 2), the pump and stirrer are stopped. After stabilization of the system, temperature and pressure signals are recorded and the PVT cell is pressurized again. The procedure is repeated three times at the same temperature and overall composition to evaluate the repeatability of the results. After that, the system temperature is changed (temperature T_2 in Fig. 2) and the procedure is repeated for the same overall composition as before (z_1). The refrigerant liquid mass fraction (solubility) at the point of phase transition is assumed equal to the overall composition ($x_1 = z_1$), as the mass of refrigerant in the vapor bubbles is very small. When

all temperature conditions are evaluated at a given composition, the latter is changed by pumping a specified amount of oil into the front chamber.

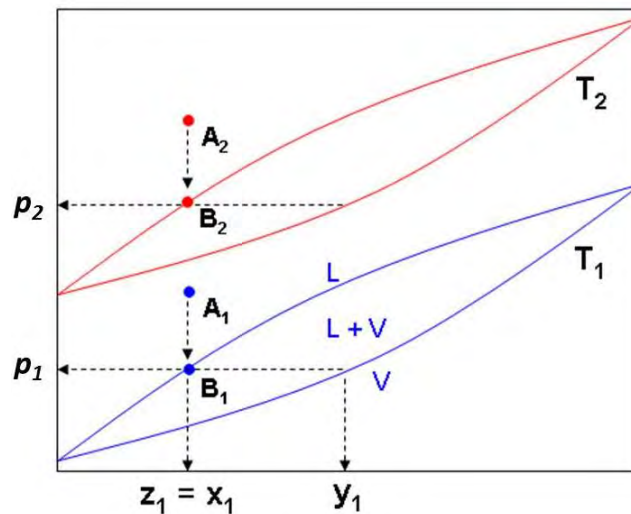


Figure 2. Schematic p - T - x - y diagram illustrating the phase transition lines in a binary mixture.

For the mixtures studied in this work, the dew point line (represented by V in Fig. 2) will be disregarded, since it is reasonable to assume that the vapor phase is comprised of pure refrigerant due to the very low vapor pressure of lubricating oils (ASHRAE, 2010).

The phase equilibrium experiments with the R-1234yf and R-134a/POE ISO VG 10 mixtures were performed at eight different temperatures (13, 20, 30, 40, 50, 60, 70 and 80°C). R-134a and R-1234yf were 99.9% pure according to their manufacturers/suppliers.

3. THERMODYNAMIC MODEL

Phase equilibria in multicomponent mixtures are characterized by an equality of component fugacities in the existing phases (Elliot and Lira, 1999). For a binary liquid-vapor mixture,

$$\hat{f}_i^L = \hat{f}_i^V \quad (1)$$

where i is a component in the mixture.

The component fugacities in both phases are calculated using a cubic equation of state (Peng and Robinson, 1976) with a classical quadratic mixing rule (Elliot and Lira, 1999). The Peng and Robinson (1976) equation of state is one of the most widely used cubic equations of state and has been successfully employed by many authors to determine the phase equilibrium in refrigerant-oil mixtures (Martz and Jacobi, 1994; Yokozeki, 2007). In terms of the compressibility factor, $Z = PV/RT$, the Peng and Robinson equation of state is given by,

$$Z^3 - (1 - B)Z^2 + (A - 3B^3 - 2B)Z - (AB - B^2 - B^3) = 0 \quad (2)$$

where A and B are dimensionless parameters given by,

$$A = \frac{ap}{R^2T^2} \quad (3)$$

$$B = \frac{bp}{RT} \quad (4)$$

and:

$$a(T) = \sum_{i=1}^n \sum_{j=1}^n \bar{x}_i \bar{x}_j a_{ij} \quad (5)$$

$$b = \sum_{i=1}^n \bar{x}_i b_i \quad (6)$$

$$(a_{ij})_{i \neq j} = \sqrt{a_i a_j} (1 - k_{ij}) \quad (7)$$

$$a_i = 0.45723553\alpha \frac{R^2 T_c^2}{p_c} \quad (8)$$

$$b_i = 0.07779607 \frac{RT_c}{p_c} \quad (9)$$

$$\alpha = [1 + (0.37464 + 1.54226\omega - 0.26993\omega^2)(1 - \sqrt{T_R})]^2 \quad (10)$$

The binary interaction parameter, k_{ij} , was adjusted to best fit the experimental data. The fugacity coefficient of component i in each phase is calculated via the Gibbs energy departure function (Elliot and Lira, 1999) as follows,

$$\ln \hat{\phi}_i = \ln \left(\frac{\hat{f}_i}{\bar{x}_i p} \right) = \frac{b_i}{b} (Z - 1) - \ln (Z - b) - \frac{a(T)}{2\sqrt{2}b} \left(\frac{2}{a(T)} \sum_{j=1}^n \bar{x}_i a_{ij} - \frac{b_i}{b} \right) \ln \left(\frac{Z + 2.414b}{Z - 2.414b} \right) \quad (11)$$

where \bar{x}_i is the component mole fraction in each phase. As the vapor pressure of the lubricant oil is negligible it can be assumed that the vapor mole fraction of refrigerant equals unity. Eq. (11) can be used to calculate the fugacity coefficients in the liquid and vapor phases.

Iterative calculation procedures (Elliot and Lira, 1999; Assael *et al.*, 1998) were applied to solve Eq. (1) for the vapor-liquid equilibrium (VLE). The equations were implemented in the Engineering Equation Solver (EES) program (Klein, 2013). Pure component constants for the refrigerant were obtained from the physical properties database embedded in EES. The acentric factor and critical properties of the oil were calculated using the group contribution method of Constantinou and Gani (1994), which provided the following values: $T_c = 595.8^\circ\text{C}$, $p_c = 6.92$ bar and $\omega = 1.0659$.

4. RESULTS

The experimental apparatus was validated with bubble pressure measurements of pure R-134a (99.5% pure) up to the critical point. Figure 3 presents a comparison between the experimental and the reference data. The reference data for bubble pressure of R-134a were calculated from EES (Klein, 2013). The measurements are within the precision level stated by the pressure transducer manufacturer. The average absolute deviation (AAD) is 0.9055%.

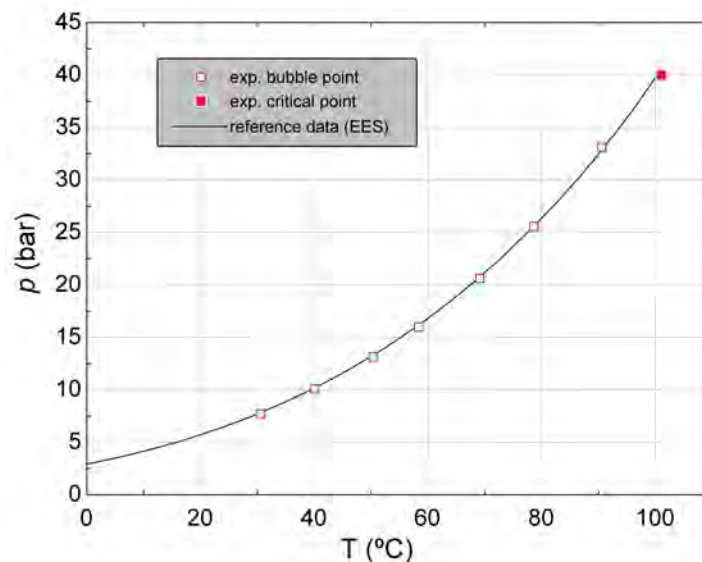


Figure 3. Validation of experimental procedure with R-134a (comparison with reference data).

Figure 4 shows a sequence of four photographs taken around the critical point of R-134a. In a state of vapor-liquid equilibrium (Fig. 4a), the temperature was maintained close to the critical temperature of R-134 (101°C) while the pressure was increased (Fig. 4b and Fig. 4c). It can be observed that the interface between the liquid and vapor phases disappears (Fig. 4d) when the system pressure reaches the critical pressure.

A phase equilibrium diagram (p - T - x) of the R-1234yf/POE ISO VG 10 mixture is shown in Fig. 5. In total, 48 experimental data points were measured. The system exhibited vapor-liquid equilibrium (VLE) and complete miscibility occurred over the entire temperature and composition ranges. Raoult's law, which characterizes the behavior of an ideal solution, has also been used to correlated the phase behavior of the mixture. According to Raoult's law, the partial pressure

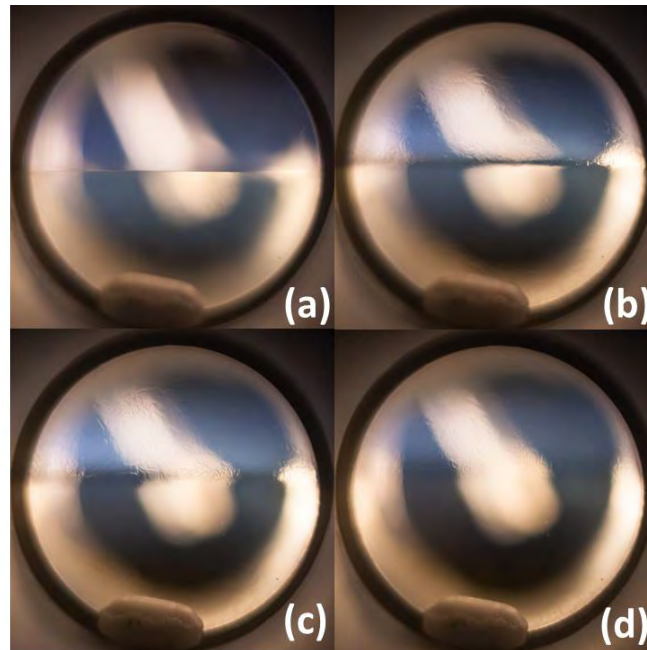


Figure 4. Sequence of images taken close to the critical point of R-134a.

of each component in the ideal mixture is dependent of the individual components bubble pressure and the molar fraction of these components. As for refrigerant-oil mixtures the mole fraction of refrigerant is approximately equal to one ($\bar{y}_1 = 1$), since the oil is not volatile, the Raoult's law is,

$$p = \bar{x}_1 p_1^{sat} \quad (12)$$

where p_1^{sat} is the saturation or bubble pressure of component 1. Here 1 stands for refrigerant and 2 for oil.

The Raoult's law correlated the phase equilibria of this mixture with AAD of 6.43%, as can be observed in Fig. 5. The ideal model presented a good agreement with the experimental data up to 50°C but exhibited significant deviations at higher temperatures. The Peng and Robinson (1976) EoS correlated the phase equilibria with AAD of 3.53% (Fig. 5). A good agreement over the whole pressure and temperature ranges is observed, indicating the suitability of the equation of the state/mixing rules. Figure 6 presents a comparison between the experimental and calculated bubble-point pressures predicted by the Peng and Robinson (1976) EoS and the Raoult's law for this mixture. As the pressure increases, deviations tend to intensify. However, for the Peng and Robinson (1976) EoS, the range of error goes up to 10%, which is an acceptable value for engineering applications.

In order to compare the behavior of R-1234yf and R-134a in terms of their interaction with the lubricant oil, vapor-liquid equilibrium experiments were also conducted for R-134a. Phase equilibria diagram (p - T - x) of the R-134a/POE ISO VG 10 mixture is shown in Fig. 7. The system exhibits similar phase behavior to R-1234yf/POE ISO VG 10, vapor-liquid equilibrium (VLE) and complete miscibility over the temperature and composition ranges. Nevertheless, it is seen that R-1234yf is more soluble in the POE ISO VG 10 oil than the R-134a. Raoult's law correlated the phase equilibria of this mixture with AAD of 5.25%, as can be observed in Fig. 7. The Peng and Robinson (1976) EoS correlated the phase equilibria with average AAD of 3.22%. Figure 8 presents a comparison between the experimental and calculated bubble-point pressures predicted by the Peng and Robinson (1976) EoS and the Raoult's law for this mixture. A summary of the statistical quantities and the parameters of the PR EoS for both systems can be observed in Table 1. It is noticeable that the PR EoS improved the correlation of the experimental data for both systems.

5. CONCLUSIONS

Due to the lack of available data on phase equilibrium for the R-1234yf/oil system, a PVT cell was utilized to measure the vapor-liquid equilibrium behavior of the mixture. The experimental apparatus was initially validated with pure refrigerant and the principal findings of this study are as follows:

- The mixtures R-134a/POE ISO VG 10 and R-1234yf /POE ISO VG 10 exhibited similar phase behavior, with vapor-liquid equilibrium being observed over the entire range of temperatures and compositions. However, R-1234yf was more soluble in the POE ISO VG 10 oil than the R-134a. No miscibility gaps were identified in the temperature range covered by the experiments;

Rafael Massabki França, Moisés A. Marcelino Neto and Jader R. Barbosa Jr.
Phase Equilibrium Data and Thermodynamic Modeling of the System R-1234yf and Polyol Ester Lubricant Oil

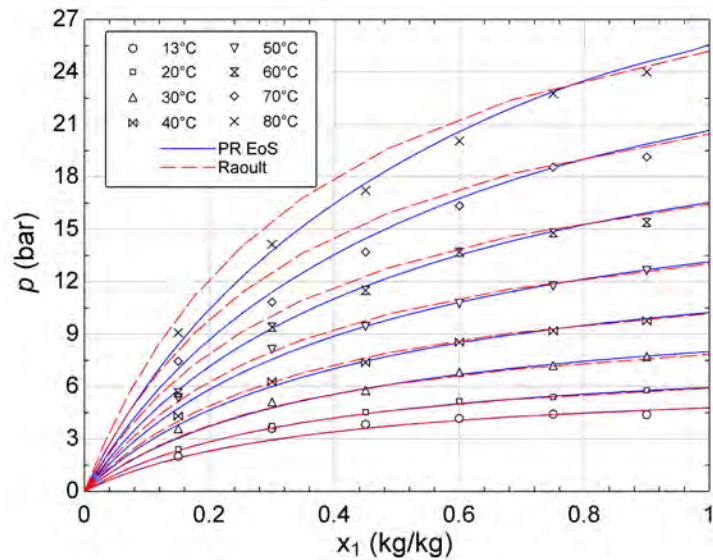


Figure 5. p - T - x diagram of the R-1234yf/POE ISO VG 10 mixture. Experimental and calculated data with Raoult's law and PR EoS.

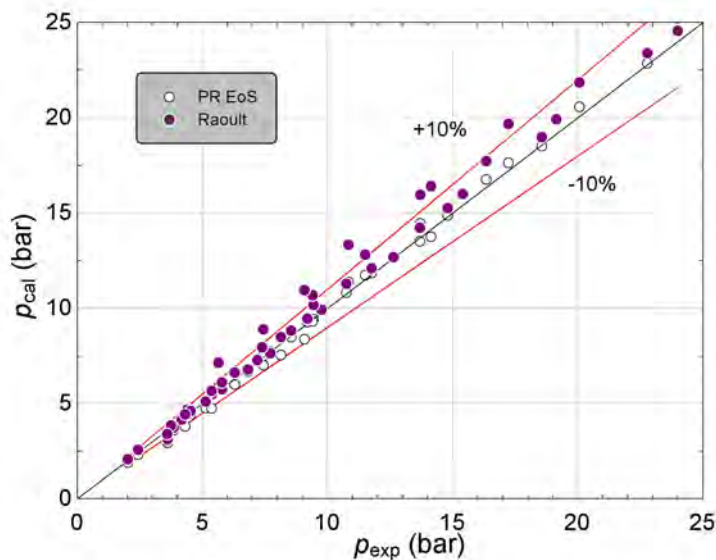


Figure 6. Comparison of bubble point pressures calculated with PR EoS and Raoult's law for R-1234yf/POE ISO VG 10 system.

Table 1. Summary of statistical quantities and model parameters.

Model	System	k_{ij}	AAD ⁽¹⁾ (%)	RMS ⁽²⁾ (%)	Bias ⁽³⁾ (%)
Raoult	R-1234yf/POE ISO VG 10	-	6.43	1.31	-5.47
	R-134a/POE ISO VG 10	-	5.25	1.00	0.29
PR EoS	R-1234yf/POE ISO VG 10	-0.009006	3.53	0.75	-1.59
	R-134a/POE ISO VG 10	-0.002851	3.22	0.74	-0.62

$$^{(1)} \text{ average absolute deviation } (AAD = \frac{100}{n} \sum_{i=1}^n \left| \frac{(x_{1,cal} - x_{1,exp})}{(x_{1,exp})} \right|)$$

$$^{(2)} \text{ root mean square } (RMS = \frac{100}{n} \sqrt{\sum_{i=1}^n \frac{(x_{1,cal} - x_{1,exp})^2}{(x_{1,exp})^2}})$$

$$^{(3)} \text{ bias } (Bias = \frac{100}{n} \sum_{i=1}^n \frac{(x_{1,cal} - x_{1,exp})}{x_{1,exp}})$$

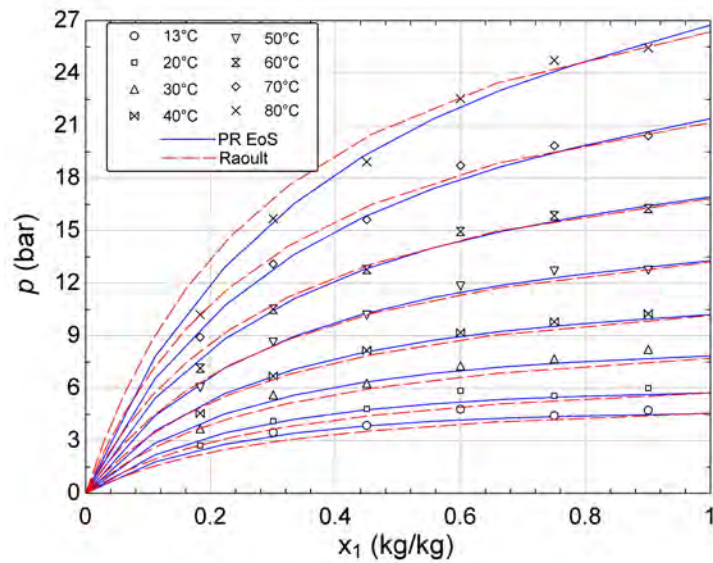


Figure 7. p - T - x diagram of of the R-134a/POE ISO VG 10 mixture. Experimental and calculated data with Raoult's law and PR EoS.

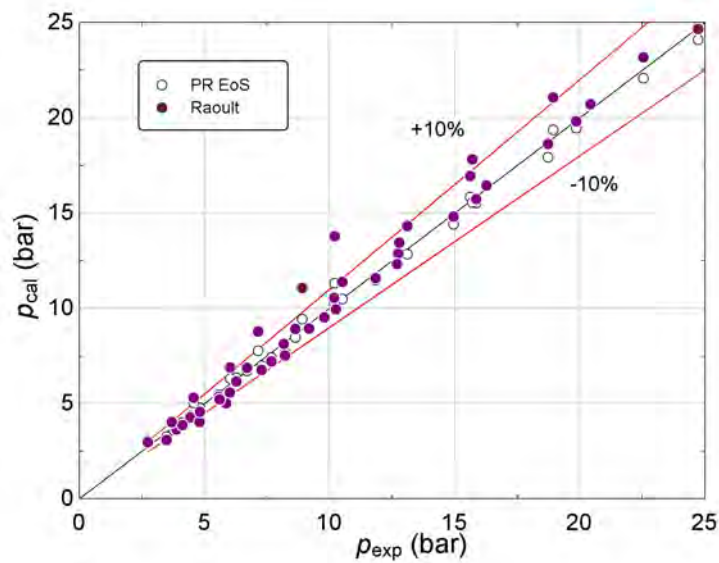


Figure 8. Comparison of bubble point pressures calculated with PR EoS and Raoult's law for R-134a/POE ISO VG 10 system.

- The conformity of Raoult's law to the experimental data is quite remarkable, indicating a small departure from ideal mixture behavior mainly at low pressures and temperatures;
- The relationship between bubble pressure, solubility and temperature was predicted with success by the fugacity coefficient model using the Peng and Robinson (1976) EoS and the quadratic mixing rules.

6. ACKNOWLEDGEMENTS

The authors thank Pedro M. de Oliveira for the photographs of the critical point.

7. REFERENCES

- ASHRAE, 2010. "Chapter 12. Lubricants in Refrigerant Systems". In: 2010 Refrigeration Handbook. American Society of Heating, Refrigeration and Air-Conditioning Engineers, Inc.
- Assael, M.J., Trusler, J.P.M. and Tsolakis, T.F., 1998. *Thermophysical Properties of Fluids*. Imperial College Press.

Rafael Massabki França, Moisés A. Marcelino Neto and Jader R. Barbosa Jr.
Phase Equilibrium Data and Thermodynamic Modeling of the System R-1234yf and Polyol Ester Lubricant Oil

- Bobbo, S., Groppo, F., Scattolini, M. and Fedele, L., 2011. "R-1234yf as a substitute of R-134a in automotive air conditioning. Solubility measurements in commercial PAG". In *23rd IIR International Congress of Refrigeration, ICR 2011, Prague, Czech Republic, Aug. 21-26, paper 528*.
- Constantinou, L. and Gani, R., 1994. "New group contribution method for estimating properties of pure compounds". *American Institute of Chemical Engineers Journal*, Vol. 40, pp. 1697–1710.
- Elliot, J.R. and Lira, C.T., 1999. *Introductory Chemical Engineering Thermodynamics*. Prentice Hall International Series in the Physical and Chemical Engineering Science.
- Klein, S.A., 2013. "Engineering Equation Solver (EES) Professional Version". V9.339, F-Chart Software, Madison, WI.
- Leck, T., 2009. "Evaluation of HFO-1234yf as a replacement for R-134a in refrigeration and air conditioning applications". In *3rd IIR Conference on Thermophysical Properties and Transfer Processes of Refrigerants, Boulder, USA, paper IIR-155*.
- Martz, W.L. and Jacobi, A.M., 1994. *Refrigerant-oil mixtures and local composition modeling*. Master's thesis, University of Illinois at Urbana-Champaign.
- Peng, D.Y. and Robinson, D.B., 1976. "A new two-constant equation of state". *Industrial & Engineering Chemistry Research*, Vol. 15, pp. 59–64.
- Spatz, M., 2009. "HFO-1234yf technology update - part II". In *VDA Winter Meeting, Saalfelden, Austria*.
- Yokozeki, A., 2007. "Solubility correlation and phase behaviours of carbon dioxide and lubricant oil mixtures". *Applied Energy*, Vol. 84, pp. 159–175.
- Zilio, C., Brown, J.S., Schiochet, G. and Cavallini, A., 2011. "The refrigerant R-1234yf in air conditioning systems". *Energy*, Vol. 36, pp. 6110–6120.

8. RESPONSIBILITY NOTICE

The authors are the only responsible for the printed material included in this paper.